

A Study of Higher Order Volume Scattering in a Layer of Discrete Random Scatterers

Muhamad Jalaluddin Jamri^a, Syabeela Syahali^b and Dina Naqiba Nur Ezzaty Abd Wahid^c
Faculty of Engineering and Technology, Multimedia University, Melaka, Malaysia

Keywords: Remote Sensing, Volume Scattering, Backscattering Coefficient, Discrete Random Scatterers, Radiative Transfer Equation.

Abstract: Remote sensing has been widely used as an earth observation technique to study the polar region. Volume scattering process is one of the scattering processes that occur in a layer of discrete random scatterers in remote sensing. In certain layer, volume scattering is significant and important to determine the value of backscattering coefficient. Previous study modelled the volume scattering only for first and second order. In this paper, a third order volume backscattering coefficient formulation is derived and added into the theoretical modelling of volume scattering, and its backscattering coefficient is analysed for different types of layer configuration embedded with discrete random scatterers. The condition of which the third order volume scattering may be important is studied. Results show that, third order volume scattering activity is significant when the scatterers in the layer are larger and with higher permittivity in both lower and higher incident angles, for all the frequency range studied.

1 INTRODUCTION

In recent years, there has been a lot of interest in the use of microwave remote sensing (Boerner, Mott, & Luneburg, 1997; Guo, Jia, & Paull, 2017; Xiong & Shi, 2017) for a layer of discrete random scatterers such as sea ice (Syahali & Ewe, 2013), snow (Syahali & Ewe, 2016) and oil palm (Toh, Ewe, Tey, & Tay, 2019). It is interesting and important to model and calculate the interaction of the electromagnetic wave with the medium, as the backscattering returns from the medium will be recorded and processed. Hence, it is important to model the scattering process as accurately as possible, and reliable to be used in certain conditions. In modelling the scattering process in an electrically dense medium where the average separation between the scatterer is comparable to the wavelength (Ewe & Chuah, 1998a), there are three types of scattering involved, which are surface scattering, surface-volume scattering and volume scattering (Syahali & Ewe, 2013, 2016). For volume scattering, the scattering terms included to calculate the backscattering coefficient was up to the second

order volume backscattering (Ewe, Chuah, & Fung, 1998b), which limits the scatterers involved in the mechanism to only two scatterers. However, for certain medium where volume scattering activity may be dominating, higher order volume scattering may be significant, therefore, more term needs to be derived and added in the formulation.

Radiative transfer theory (Chandrasekhar, 1960; Tsang, Kubacsi, & Kong, 1981) had been identified as the form of electromagnetic radiation between medium. Therefore, theoretical model for an electrically dense medium based on the radiative transfer theory was developed to calculate and study the scattering mechanisms. The dense medium was constructed as a layer randomly embedded with distributed spherical scatterers in a homogenous medium and based on (Mao-yan, Jun, Jian, & Hailong, 2007) the spherical scatterer is modelled as a Mie scatterer. The parameters such as frequency, scatterer radius, permittivity of the scatterer and incident angle are some of the factors that determine the volume backscattering from these scatterers.

^a  <https://orcid.org/0000-0003-2273-3232>

^b  <https://orcid.org/0000-0002-6847-8591>

^c  <https://orcid.org/0000-0002-6982-8549>

In this paper, a third order volume backscattering coefficient formulation is derived from the Radiative Transfer Theory equation by using the iterative method (Tsang et al, 1981;Karam, Fung, Lang, & Chauhan, 1992) and inspection of its backscattering coefficient is done for layers with different scatterer permittivity and size, and using different frequency and incident angle of the wave. The performance of backscattering coefficient mainly depends on these parameters and the condition of which the third order volume scattering is significant and may contribute to the total backscattering coefficient values are analysed and discussed before the research is concluded. This research is important to determine the condition which the higher order volume scattering may be important and should be included in theoretical modelling, as reference for researchers working in this area.

2 METHODOLOGY

2.1 Model Configuration

Figure 1 shows a cross section of the layer used in theoretical modelling (Ewe & Chuah, 1997). The layer is modelled as a discretely inhomogeneous medium of depth d (in m), in which randomly distributed spherical scatterers are embedded in a homogenous medium. This layer is bounded on top and bottom by irregular surface boundaries. Above the layer is air, and below is a homogeneous half space.

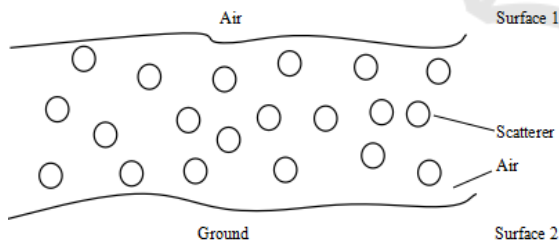


Figure 1: Cross section of the layer.

The Radiative Transfer Equation from (Chandrasekhar, 1960) characterizes the propagation and scattering of specific intensity inside a medium and is given by

$$\cos \theta \frac{d\bar{I}}{dz} = -\bar{K}_e \bar{I} + \int \bar{P} \bar{I} d\Omega \quad (1)$$

where \bar{I} is the Stokes vector, \bar{K}_e is the extinction matrix, and \bar{P} is the phase matrix of the medium (Tsang, Kong, & Shin, 1985).

The phase matrix \bar{P} is associated with the first two Stokes' parameters of the scatterers and is given in (2). θ' and ϕ' in this equation are the polar and azimuth angle before scattering, while ϵ and ϕ are the polar and azimuth angle after scattering. $\langle |\psi|^2 \rangle_n$ is the Dense Medium Phase Correction Factor (Chuah, Tjuatja, Fung, & Bredow, 1996) and \bar{S} is the Stokes' matrix for Mie scatterers with close spacing amplitude correction (Fung & Eom, 1985). $\langle |\psi|^2 \rangle_n$ is the correction factor that needs to be included into the phase matrix to take into account the coherent effect of the scattering of the closely spaced scatterers in an electrically dense medium.

$$\bar{P}(\theta, \phi; \theta', \phi') = \langle |\psi|^2 \rangle_n \cdot \bar{S} = \begin{bmatrix} P_{vv} & P_{vh} \\ P_{hv} & P_{hh} \end{bmatrix} \quad (2)$$

In (Ewe et al, 1998b), this radiative transfer equation was solved up to second order solutions. Zeroth order solutions characterize the scattering process without any scatterer involved whereas first and second order solutions characterize the scattering process involving one and two scatterers. Through this iterative solution, many scattering terms were derived and calculated. The scattered intensity I is related with the backscattering coefficient, by this formula

$$\sigma_{pq} = \frac{4\pi \cos \theta_s I_{sp}}{I_{iq}} \quad (3)$$

2.2 Theoretical Modelling

After solving (1) iteratively, the third order solution is given by

$$I_3^+(0, \theta, \phi) = R_{12}(\theta, \pi - \theta) S_2^-(-d, \pi - \theta, \phi) e^{-K_e^+ \sec \theta(d)} + S_2^+(0, \theta, \phi) \quad (4)$$

where I_3^+ is the upward intensity, R the reflectivity matrix, d the depth of the layer, K_e the volume extinction coefficient, and S_2^- and S_2^+ are the downward and upward scattered intensities.

The second term of (4) describes upward scattered intensity from the third scatterer. One of the scattering

mechanisms which can be derived from this term is illustrated in Figure 2, where the incident intensity is being transmitted from outer layer to inner layer of the medium through the upper boundary and hits the first scatterer. Then, the scattered downward intensity hits the second scatterer and scattered upward before hitting the third scatterer. Finally, it is scattered into upward direction of angle θ_{1s} .

In this study, the derived volume backscattering term from the third order solution depicted in Figure 2 is shown in (5) through (6) and describes the intensity being scattered by three scatterers. The arguments in the left hand side of the equation describes the upward and downward directions of the intensity throughout the scattering process, starting from the right to left.

$$\sigma_{3,pq}(up, up, down, down) = \frac{4\pi \cos \theta_s I_{3pq}^+(\theta_s, \phi_s; \pi - \theta_i, \phi_i)}{I_i} \quad (5)$$

$$= 4\pi \cos \theta_s T_{01}(\theta_s, \theta_{1s}) T_{10}(\pi - \theta_{1i}, \pi - \theta_i) \sec \theta_{1s}$$

$$\int_0^{\frac{\pi}{2}} \int_0^{\frac{\pi}{2}} \int_0^{\frac{\pi}{2}} \int_0^{\frac{\pi}{2}} \sec \theta'' \sin \theta'' d\theta'' d\phi'' \sec \theta' \sin \theta' d\theta' d\phi'$$

$$\sum_{t=v,h} \sum_{u=v,h} P_3(\theta_{1s}, \phi_{1s}; \theta', \phi') P_2(\theta', \phi'; \pi - \theta'', \phi'')$$

$$P_1(\pi - \theta'', \phi''; \pi - \theta_{1i}, \phi_{1i})$$

$$\left[\begin{array}{l} \frac{L_u^-(\theta'') - L_q^-(\theta_{1i}) L_t^+(\theta')}{K_{eq}^- \sec \theta_{1i} - K_{eu}^- \sec \theta'' - K_{et}^+ \sec \theta'} \\ \frac{1 - L_p^+(\theta_{1s})}{(K_{et}^+ \sec \theta')(K_{ep}^+ \sec \theta_{1s})} - \frac{L_t^+(\theta') - L_p^+(\theta_{1s})}{(K_{et}^+ \sec \theta')(K_{ep}^+ \sec \theta_{1s}) - K_{et}^+ \sec \theta'} \end{array} \right]$$

(6)

where θ_{1s} and θ_{1i} are the scattered angle and incident angle, respectively, in the random layer through the Snell's Law while θ_s and θ_i are the angles outside the layer. θ'' and θ' are the scattered angles in the layer during the scattering processes with the scatterer. p and q are the scattered polarization and incident polarization, respectively

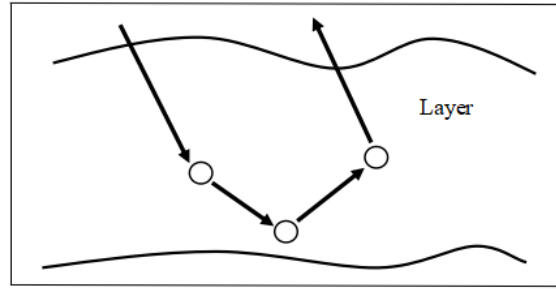


Figure 2: Scattering mechanisms from the term of Equation 6.

while u and t are the polarization during the scattering processes in the layer.

I_i is the incident intensity while T_{10} and T_{01} are the transmittivity from top boundary into the layer, and from layer into the top boundary, respectively. P is the phase matrix of the medium, and K_e is the volume extinction coefficient. L with positive and negative superscripts describe the attenuation of upward and downward intensities, respectively, and is given by

$$L_u^-(\theta) = e^{-K_{eu}^+ \sec \theta d} \quad (7)$$

After all, only $S_2^+(0, \theta, \phi)$ from (4) is taken into account due to the dominant impact for volume scattering process.

3 RESULT AND DISCUSSION

Theoretical analysis is done by applying the third order volume backscattered coefficient solution to a layer of discrete random scatterers. Based on (Fung & Eom, 1985) and (Chuah, Tjuatja, Fung, & Bredow, 1997), any layer containing spherical scatterers treated as an inhomogeneous medium. In performing the third order volume backscattering calculation, volume backscattering terms is calculated by the model simulation written in FORTRAN software. This is useful to examine in detail each backscattering mechanism in the media. The model is programmed to allow the inputs of various physical parameters so that it gives flexibility in simulating the model for different parameters, such as frequency, permittivity of the scatterers, incident angle of the wave and scatterer radius.

The input parameters used are based on (Syahali & Ewe, 2016) and listed in Table 1. The third order volume scattering is calculated for different polarization and different input parameters, over a range of frequency from 4 GHz to 14 GHz. The effect

of permittivity, incident angle and scatterer radius on the contribution of third order volume scattering is investigated. This is done by varying the permittivity, incident angle and scatterer radius of the inhomogeneous medium.

Table 1: Model parameters used in theoretical analysis.

Parameter	Estimated Values
Incident angle	10°
Scatterer Radius/mm	0.5
Volume fraction/%	30
Effective relative permittivity of top layer	(1.0, 0.0)
Relative permittivity of sphere	(2, 0.001)
Background relative permittivity	(1.0, 0.0)
Lower half-space permittivity	(5.0, 0.0)
Thickness of layer/m	0.5
Top surface rms height and correlation length/cm	0.14, 0.7

To investigate the effect for different incident angles, the incident angle is first varied from 10° to 20° and 30°. The third order volume backscattering return is observed against frequency for co-polarized (VV) and cross polarized (VH) wave return. The pattern shows that the third order volume backscattering coefficient is increasing along with the frequency. This is because the albedo increases as frequency increases (Fung, 1994; Fung & Chen, 2010).

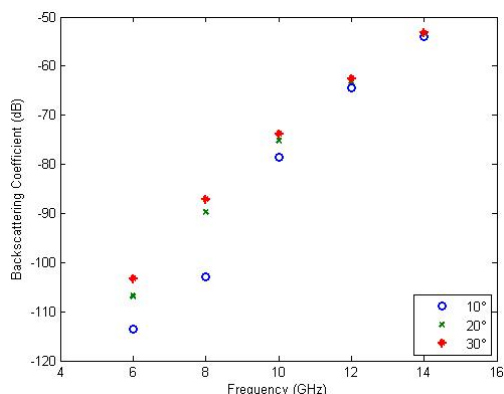


Figure 3: Third order volume scattering coefficient (VV polarization) against frequency for various incident angle.

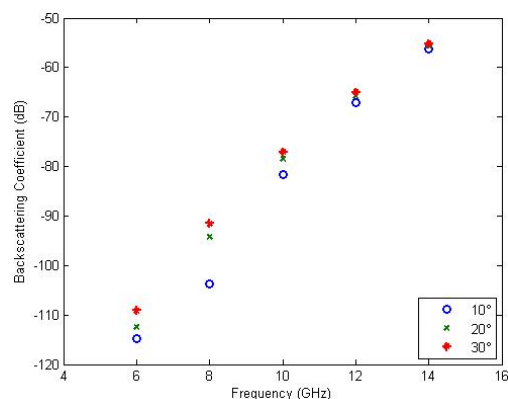


Figure 4: Third order volume scattering coefficient (VH polarization) against frequency for various incident angle.

It can also be seen that the third order volume backscattering coefficient increases when the incident angle is increased. To study this effect in more detail, Figure 5 shows the plot of third order volume backscattering coefficient (VV polarization) against incident angle for various frequency. It can be observed that the increment of the backscattering coefficient with incident angle mainly occurs at low frequency. The reason may be due to longer wavelength responding more with change in incident angles because of its ability to penetrate deeper into the layer. This suggests that higher order volume scattering is more significant when the wave used is of higher frequency.

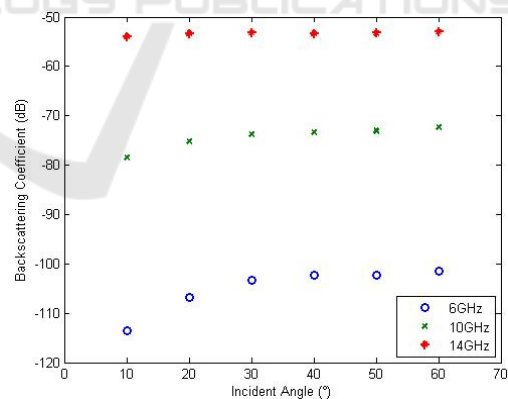


Figure 5: Third order volume scattering coefficient (VV polarization) against incident angle for various frequency.

Next, for permittivity of the scatterer, the real part is varied from 2 to 3 and 4 while the imaginary part remains constant. Then, the third order volume backscattering return for each input permittivity is plotted for co-polarized (VV) and cross polarized (VH) return over the frequency of 4 GHz to 14 GHz in Figure 6 and 7. For co-polarized (VV) and cross

polarized (VH) return, the pattern shows that third order volume backscattering coefficient is increasing along with the frequency for all the permittivity values used. It can also be seen that the third order volume backscattering coefficient increases when the permittivity is increased in this range of frequency. Higher permittivity increases the visibility of the scatterers in the medium and this may have increased the volume scattering activity. This shows that the third order volume scattering is significant in the area where the scatterers have high permittivity values.

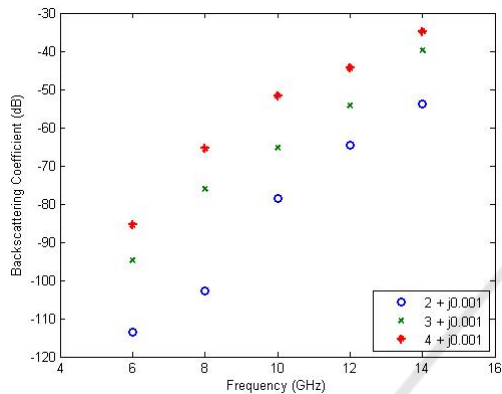


Figure 6: Third order volume scattering coefficient (VV polarization) against frequency for various permittivity of scatterers.

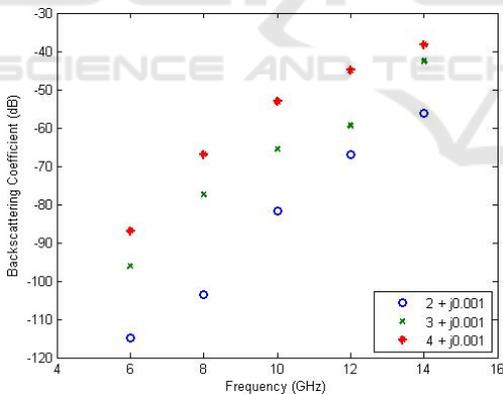


Figure 7: Third order volume scattering coefficient (VH polarization) against frequency for various permittivity of scatterers.

In Figure 8 and 9, variation of the size of the discrete random scatterers is shown for co-polarized (VV) and cross polarized (VH), where the value for the radius is varied from 0.5 mm to 0.75 mm and 1.0 mm for backscattering return over frequency 4 GHz to 14 GHz. Results show that larger particles cause greater backscattering return in like and cross polarization. As with the permittivity, the improved scatterer's visibility due to larger size may have

improved the third order volume backscattering coefficient, suggesting the importance of higher order volume scattering in the medium filled with large scatterers. It can also be seen for both polarized return that the third order volume backscattering is increasing with frequency for all the scatterer radius used.

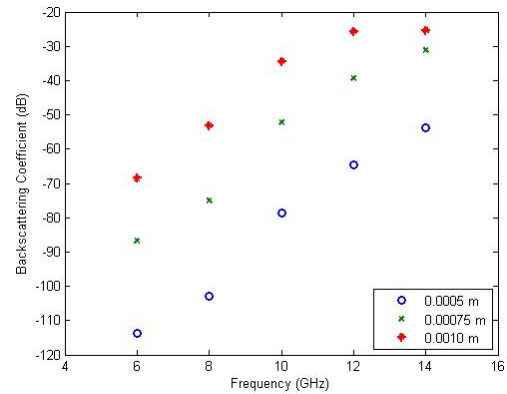


Figure 8: Third order volume scattering coefficient (VV polarization) against frequency for various radius of scatterers.

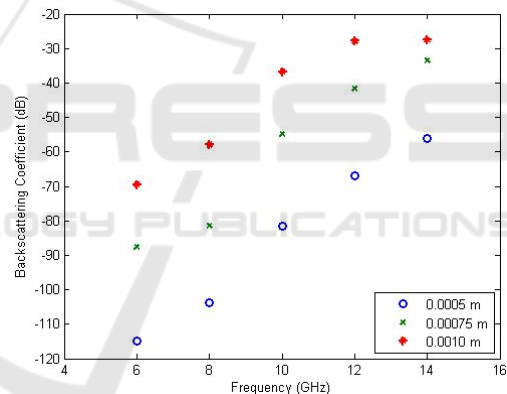


Figure 9: Third order volume scattering coefficient (VH polarization) against frequency for various radius of scatterers.

Lastly, to further analyse the contribution of higher order volume scattering, analysis is done on the backscattering coefficient of different orders of volume scattering in a larger frequency range. Figure 10 shows the plot of volume backscattering coefficient (VV polarization) against frequency for first, second and third order volume scattering. It shows that after 15 GHz, volume scattering is dominated by first and second order scattering. Therefore, higher order volume scattering is not significant at this frequency range, to determine the value of backscattering coefficient, because the third order backscattering coefficient started to disappear at high frequency.

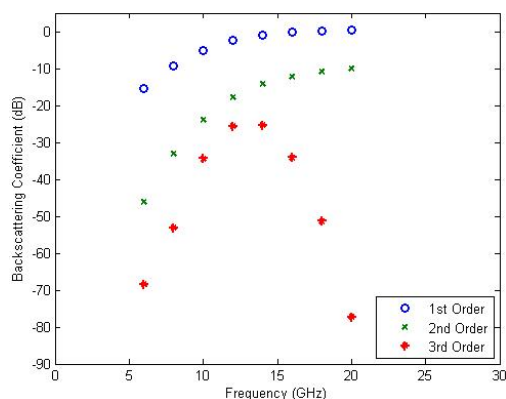


Figure 10: Volume scattering coefficient (VV polarization) against frequency for different order backscattering coefficient.

4 CONCLUSIONS

In this paper, third order volume scattering is derived and presented. Theoretical analysis shows that there is an increase in the pattern of the third order volume backscattering coefficient as the frequency of the wave used gets higher, and when the radius and permittivity of scatterers in the layer are larger. This suggests that higher order volume scattering is significant and should be considered in developing theoretical modelling in these areas. However, further study in higher frequency range shows that after 15 GHz, volume scattering is dominated by first and second order volume scattering, indicating that higher order volume scattering is no more significant at very high frequency range. In future, this model may be further improved by considering more third order volume scattering terms and by incorporating numerical solution model in the phase matrix calculation (Lum, Ewe, & Jiang, 2015; Lum, Fu, Ewe, Jiang, & Chuah, 2017a; Lum, Fu, Ewe, & Jiang, 2017b; Syahali, Ewe, Vetharatnam, Jiang, & Kumaresan, 2020).

REFERENCES

- Boerner, W. , Mott, H., & Luneburg, E. (1997). Polarimetry in remote sensing: basic and applied concepts. *IGARSS'97. 1997 IEEE International Geoscience and Remote Sensing Symposium Proceedings. Remote Sensing - A Scientific Vision for Sustainable Development*, 3, pp. 1401-1403 vol.3.
- Chandrasekhar, S. (1950). 1960, Radiative Transfer. *Dever, New York*.
- Chuah, H. T., Tjuatja, S., Fung, A. K., & Bredow, J. W. (1996). A phase matrix for a dense discrete random medium: Evaluation of volume scattering coefficient. *IEEE Transactions on Geoscience and Remote Sensing*, 34(5), 1137-1143.
- Chuah, H. T., Tjuatja, S., Fung, A. K., & Bredow, J. W. (1997). Radar backscatter from a dense discrete random medium. *IEEE transactions on geoscience and remote sensing*, 35(4), 892-900.
- Ewe, H. T., & Chuah, H. T. (1997, August). A study of dense medium effect using a simple backscattering model. In *IGARSS'97. 1997 IEEE International Geoscience and Remote Sensing Symposium Proceedings. Remote Sensing-A Scientific Vision for Sustainable Development* (Vol. 3, pp. 1427-1429). IEEE.
- Ewe, H. T., & Chuah, H. T. (1998a, July). An analysis of the scattering of discrete scatterers in an electrically dense medium. In *IGARSS'98. Sensing and Managing the Environment. 1998 IEEE International Geoscience and Remote Sensing Symposium Proceedings. (Cat. No. 98CH36174)* (Vol. 5, pp. 2378-2380). IEEE.
- Ewe, H. T., Chuah, H. T., & Fung, A. K. (1998b). A backscatter model for a dense discrete medium: Analysis and numerical results. *Remote Sensing of Environment*, 65(2), 195-203.
- Fu, X., Jiang, L. J., & Ewe, H. T. (2016). A novel relaxed hierarchical equivalent source algorithm (RHESA) for electromagnetic scattering analysis of dielectric objects. *Journal of Electromagnetic Waves and Applications*, 30(12), 1631-1642.
- Fung, A. K. (1994). Microwave scattering and emission models and their applications. *Norwood, MA: Artech House, 1994*.
- Fung, A. K., & Eom, H. J. (1985). A study of backscattering and emission from closely packed inhomogeneous media. *IEEE transactions on geoscience and remote sensing*, (5), 761-767.
- Fung, A. K. & Chen, K. S. (2010). *Microwave scattering and emission models for users*. Artech house.
- Guo, Y., Jia, X., & Paull, D. (2017). Sequential classifier training for rice mapping with multitemporal remote sensing imagery. *ISPRS Annals of the Photogrammetry, Remote Sensing and Spatial Information Sciences*, 4, 161.
- Karam, M. A., Fung, A. K., Lang, R. H., & Chauhan, N. S. (1992). A microwave scattering model for layered vegetation. *IEEE Transactions on Geoscience and Remote Sensing*, 30(4), 767-784.
- Lum, C. F., Ewe, H. T., Xin, F., Jiang, L. J., & Chuah, H. T. (2017a, July). An analysis of scattering from snow with relaxed hierarchical equivalent source algorithm. In *2017 IEEE International Geoscience and Remote Sensing Symposium (IGARSS)* (pp. 1434-1437). IEEE.
- Lum, C. F., Ewe, H. T., & Jiang, L. J. (2015, December). A study of single scattering of scatterer at various orientation angles with equivalence principle algorithm. In *2015 10th International Conference on Information, Communications and Signal Processing (ICICS)* (pp. 1-4). IEEE.

- Lum, C. F., Fu, X., Ewe, H. T., & Jiang, L. J. (2017b). A study of scattering from snow embedded with non-spherical shapes of scatterers with Relaxed Hierarchical Equivalent Source Algorithm (RHESA). *Progress In Electromagnetics Research*, 61, 51-60.
- Mao-yan, W., Jun, X., Jian, W., & Hai-long, L. (2007, October). Mie Series Study on Electromagnetic Scattering of Metallic Sphere Covered by Double-negative Metamaterials. In *2007 International Symposium on Electromagnetic Compatibility* (pp. 482-485). IEEE.
- Syahali, S., & Ewe, H. T. (2013). Remote sensing backscattering model for sea ice: Theoretical modelling and analysis. *Advances in Polar Science*, 24(4), 258-264.
- Syahali, S., & Ewe, H. T. (2016). Backscattering analysis for snow remote sensing model with higher order of surface-volume scattering. *Progress In Electromagnetics Research*, 48, 25-36.
- Syahali, S., Ewe, H. T., Vetharatnam, G., Jiang, L. J., & Kumaresan, H. A. (2020). Backscattering Analysis of Cylinder Shaped Scatterer in Vegetation Medium: Comparison Between Theories. *Journal of Engineering Technology and Applied Physics*, 2(1), 15-18..
- Toh, C. M., Ewe, H. T., Tey, S. H., & Tay, Y. H. (2019). A study on oil palm remote sensing at l-band with dense medium microwave backscattering model. *IEEE Transactions on Geoscience and Remote Sensing*, 57(10), 8037-8047.
- Tsang, L., Kong, J. A., & Shin, R. T. (1985). Theory of microwave remote sensing(Book). *Research supported by the Schlumberger-Doll Research Center, NSF, NASA, Navy, et al. New York, Wiley-Interscience, 1985, 627 p.*
- Tsang, L., Kubacsi, M. C., & Kong, J. A. (1981). Radiative transfer theory for active remote sensing of a layer of small ellipsoidal scatterers. *Radio Science*, 16(03), 321-329.
- Xiong, C., & Shi, J. (2017, July). A new snow light scattering model and its application in snow parameter retrieval from satellite remote sensing. In *2017 IEEE International Geoscience and Remote Sensing Symposium (IGARSS)* (pp. 1473-1476). IEEE.